JOURNAL OF SOLID STATE CHEMISTRY 5, 291–299 (1972)

A Study of the β→α Phase Transition in $UO_2(OH)_2$ by Dilatometric, Microcalorimetric and X-Ray Diffraction Techniques

J. C. TAYLOR, J. W. KELLY, AND B. DOWNER

A.A.E.C. Research Establishment, Lucas Heights, New South Wales, Australia

Received September 30, 1971

When β-$UO_2(OH)_2$ is cooled to about 5°C, it transforms rapidly into α-$UO_2(OH)_2$ with a volume change $\Delta V/V$ of −14.7%. The volume change was measured by dilatometry. The enthalpy change accompanying the transformation was measured by a specially constructed microcalorimeter, and found to be 1.36 ± 0.22 kcal/mole. The temperature of the transition was 5.1 ± 2.3°C. The fraction of β-$UO_2(OH)_2$ converted to α-$UO_2(OH)_2$ in each run was determined both by direct weighing and X-ray diffraction methods. The transformation is unusual for a nonmetallic crystal in that it is analogous to the martensitic transformations common in metals and alloys. On the basis of the known structures of the α and β phases, and morphological changes accompanying the transition, a mechanism for the transformation is proposed, and it is suggested that hydrogen bonds are probably not broken during the transformation.

Introduction

Uranyl hydroxide, $UO_2(OH)_2$, exists in two crystal forms, α and β, which can be prepared hydrothermally from UO_3 and H_2O (*1*). The coordination number of uranium is 6 in the octahedral β form, the $UO_2(OH)_2$ layers being linked by O–H···O (uranyl) hydrogen bonds (*2*, *3*). The $UO_2(OH)_2$ layers in the α form are also joined by O–H···O (uranyl) hydrogen bonds, but the coordination number of uranium is now 8, with a puckered hexagonal arrangement (*4*). The hydrogen atoms in each form have been located by neutron diffraction (*5*).

The β form transforms into the α form on application of pressure (*6*) or on cooling (*5*). The transition is interesting as it involves major structural changes. Studies of the physical changes accompanying the transformation by dilatometry, microcalorimetry and morphological examination are reported in this paper, and a mechanism is proposed on the basis of these new data and the previously determined structural details.

Material

A sample of pure β-$UO_2(OH)_2$ (the purity with respect to the β form was checked microscopically) was supplied by Dr. B. W. Edenborough, of the Department of Chemical Engineering, University of New South Wales. The dipyramidal β crystals had {001} and {111} faces, with distances of about 80–250 nm between {111} edges and 10–50 nm between {001} faces. The α-$UO_2(OH)_2$ crystals produced in the experiments described below were plate-shaped with dominant {010} faces and {111} faces around the edges. The average crystal sizes were:

β: 120 × 120 × 40 nm α: 70 × 70 × 15 nm.

The α average size was smaller, due to a certain amount of fracture during transformation. Relevant crystal data are given in Table I.

TABLE I

CRYSTAL DATA FOR α-$UO_2(OH)_2$ AND β-$UO_2(OH)_2$ AT 20°C

	α-$UO_2(OH)_2$[a]	β-$UO_2(OH)_2$[b]
a (Å)	4.2455(6)	5.6438(1)
b (Å)	10.3183(16)	6.2867(1)
c (Å)	6.8648(10)	9.9372(2)
V (Å^3)	300.7(1)	352.58(2)
D_x (g cm^{-3})	6.715(2) = ρ_α	5.7269(2) = ρ_β
Z	4	4
Space Group	*Cmca* or *C2cb*	*Pbca*

[a] This work, Philips 11.46 cm diam. camera, CuK radiation.

[b] From (*3*).

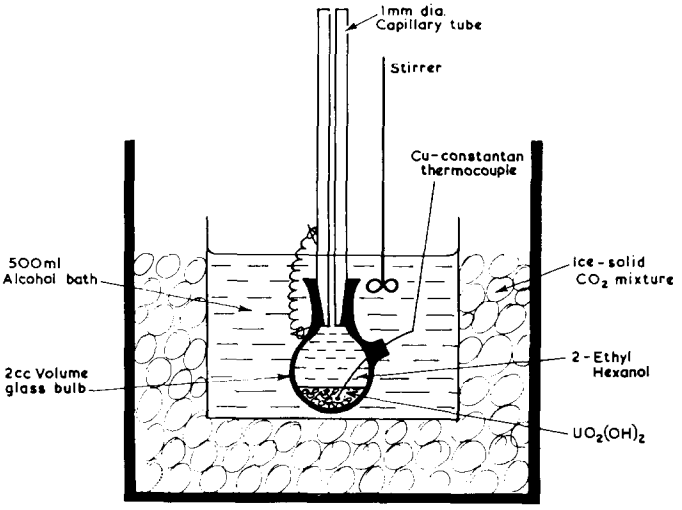

FIG. 1. Dilatometer.

Dilatometric Study

The dilatometer shown in Fig. 1 was constructed. About 0.1–0.2 g of β-$UO_2(OH)_2$ was used in each run with 2-ethylhexanol as the indicating fluid. The mean radius of the capillary was determined as 0.0552 ± 0.0002 cm (with mercury). The meniscus height was measured with a cathetometer, the transition appearing as a discontinuity in the curve of temperature vs. meniscus height, from which the contraction due to the transition and the volume change were readily calculated. Cooling rates were 0.2–0.3°C/min. A cooling curve is shown in Fig. 2.

The measured volume change $-\Delta V$ is $\pi r^2 \Delta h$ where r is the capillary radius and Δh the contraction along the capillary. The theoretical volume change is $[(1/\rho_\beta) - (1/\rho_\alpha)] \cdot mC$ where m is the initial mass of β-$UO_2(OH)_2$ and C the fraction converted to the α form. Conversion factors C were determined after each run by weighing about 0.00150 g of the product on a balance reading to ± 0.00001 g, picking out the residual β crystals under a microscope, and reweighing.

Volume contractions measured with the dilatometer are given in Table II. The mean contraction $\Delta V/V$ is $14.0 \pm 0.7\%$, in agreement with the theoretical value of 14.7%.

X-Ray Method for Determining Conversion Factors

As the direct weighing technique for determining the proportion of each phase in the product was tedious, an X-ray method of phase analysis was developed, using the dilatometric products as standards. Table III gives the direct-weighing conversion factors C for these samples, together with an independent estimate C', obtained by substituting the observed contractions into the equation for the theoretical volume change.

X-ray photographs were taken with a Guinier focusing camera using Cu$K\alpha$ radiation, and line

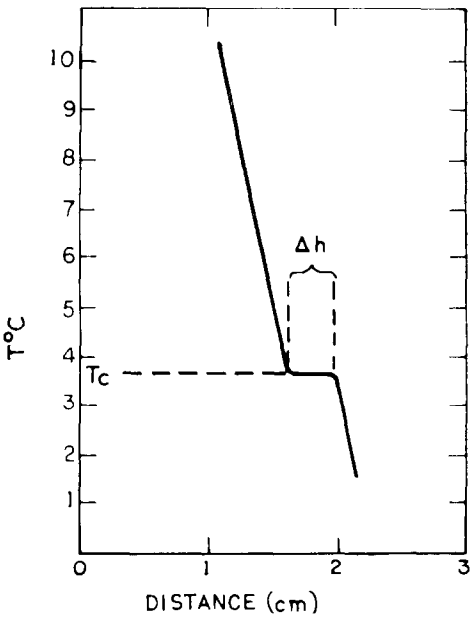

FIG. 2. Dilatometer cooling curve.

TABLE II

VOLUME CONTRACTIONS IN THE TRANSFORMATION DETERMINED BY DILATOMETRY

Sample	m (g)	Δh (mm)	$-\Delta V$ (meas) (mm³)	$V=\frac{mc}{\rho_\beta}$ (mm³)	$-\frac{\Delta V}{V}$ (%)	Transition temperature (°C)
1	0.323	5.5	5.2	38.9	13.4	8.5
2	0.105	2.4	2.3	15.5	14.8	7.0
3	0.162	3.7	3.5	26.9	13.0	3.3
4	0.186	4.5	4.3	29.2	14.7	6.0
5	0.222	4.6	4.4	31.8	13.8	0.5
6	0.229	5.0	4.8	33.2	14.5	1.3

intensities were determined with a densitometer. The usual equation for a powder line intensity is

$$I\alpha m\ N^2F^2\phi' AM\ V$$

where m is the multiplicity, N the number of unit cells of the phase per unit volume, F is the structure factor, ϕ' an angle factor consisting of the Lorentz, polarization and monochromator terms, A an absorption factor, M the temperature factor and V the volume of the diffracting crystals. The angular terms ϕ', A and M were grouped into an overall angular factor $\phi=\phi' AM$. Hence,

$$I\alpha mN^2F^2\phi(g/\rho)$$
$$\alpha mF^2\phi\rho g,$$

where g is the mass of the diffracting phase and ρ its crystal density. The X-ray conversion factor C'' thus should be

$$C''=\frac{g_\alpha}{g_\alpha+g_\beta}=\left(1+\frac{I_\beta}{I_\alpha}\cdot\frac{(mF^2\phi\rho)_\alpha}{(mF^2\phi\rho)_\beta}\right)^{-1}.$$

As the conversion factors C'' calculated from the above equation were always about 10% low, the X-ray method as it stood was unsatisfactory, being affected by systematic errors. The most probable errors were extinction and preferred orientation effects, which can be severe, but cannot be calculated theoretically. Further, the linear absorption coefficients $\mu_\alpha=1870$ cm^{-1} and $\mu_\beta=1590$ cm^{-1} for Cu$K\alpha$ radiation are very high (μ is typically 10 cm^{-1} for organic crystals). Brindley (7) has indicated that correction factors τ_α and τ_β should be applied to the two line intensities to allow for differential absorption by the two phases. Although our samples were "coarser" than the coarseness range specified by Brindley, we thought it useful to evaluate the Brindley factor τ_α/τ_β for our sample. The weighted mean $\bar{\mu}$ for the sample is $0.8\times1870+0.2\times1590=1810$ cm^{-1}, giving $(\mu-\bar{\mu})R$ values of 0.12 for the α phase and -0.77 for the β phase, where R is the average particle radius. The table on p. 195 Vol. III, of the International Tables for X-Ray Crystallography (8) gives $\tau_\alpha=0.85$ and $\tau_\beta=3.2$, or $\tau_\alpha/\tau_\beta\sim0.27$. (The table was extended from $(\mu-\bar{\mu})R=0.5$ to $(\mu-\bar{\mu})R=0.77$ for the β case.) The Brindley factor was thus in the right direction. We decided to apply a correction factor of this form, as an empirical correction was obviously necessary, keeping in mind the fact that we were probably correcting for extinction and preferred orientation effects as well. It was assumed that the systematic errors were constant for the α and β lines selected, from sample to sample, i.e. τ_α/τ_β is a constant.

The working equation now became:

$$C''=\left(1+\frac{\tau_\alpha}{\tau_\beta}\cdot\frac{I_\beta}{I_\alpha}\cdot\frac{(mF^2\phi\rho)_\alpha}{(mF^2\phi\rho)_\beta}\right)^{-1}.$$

The $\bar{C}$ values in Table III were used as standards to determine τ_α/τ_β for each sample using the

TABLE III

CONVERSION FACTORS C, C' AND C'' DETERMINED BY DIRECT WEIGHING, DILATOMETRY AND X-RAY DIFFRACTION, AND THE EXPERIMENTAL RATIOS τ_α/τ_β OF THE BRINDLEY CORRECTION FACTORS

Sample	C	C'	$\bar{C}=\frac{C+C'}{2}$	C''	τ_β/τ_β
1	0.69	0.63	0.66	0.72	0.63
2	0.85	0.85	0.85	0.73	0.23
3	0.95	0.84	0.90	0.89	0.42
4	0.90	0.89	0.90	0.86	0.36
5	0.82	0.77	0.80	0.85	0.69
6	0.83	0.81	0.82	0.84	0.55

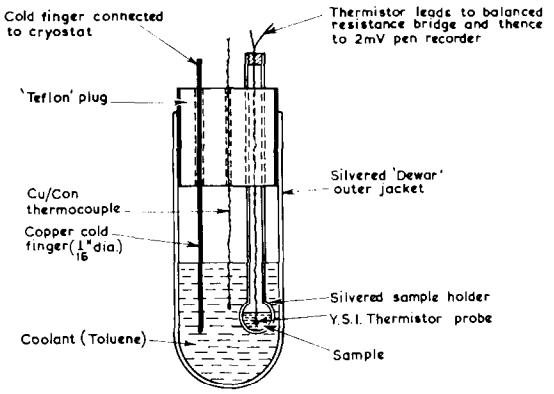

FIG. 3. Microcalorimeter.

above equation. The intensities of the β_{111} and α_{022} lines were compared. The overall angular factor ϕ was determined for each photograph by plotting I/mF^2 vs. θ for the α-phase lines (020), (022) and (113). The ϕ factor for the β_{111} line was found by interpolation. The F values included anomalous dispersion corrections. The τ_α/τ_β ratios found for each sample are given in Table III, and the mean value is 0.48 ± 0.16. Substituting the mean value for τ_α/τ_β in the above equation, X-ray conversion factors C'' were calculated for the dilatometer samples and are compared with C and C' in Table III. As good agreement was obtained, this X-ray method was considered to be satisfactory.

Calorimetric Study

Construction and Calibration of Microcalorimeter

The microcalorimeter shown in Fig. 3 was constructed to measure the heat output accompanying the transformation. The outer calorimeter was a Dewar vessel 7 cm long and 6.5 cm in diameter. A copper cold finger (connected to a cryostat), a Cu/constantan thermocouple and an inner calorimeter were fitted through the teflon plug lid. The inner calorimeter was fashioned from glass tubing (approximately 5 mm i.d.) with a small bulb at one end, and was silvered on the inside. Temperature changes in the sample (a β-$UO_2(OH)_2$–toluene mixture) were measured with a Y.S.I. thermistor probe. The thermistor probe formed one leg of a high resistance Wheatstone bridge circuit; out-of-balance voltages accompanying temperature changes in the sample were fed into a 2 mV recorder calibrated in the range -10 to $+15$°C.

The toluene coolant in the outer calorimeter was cooled by the copper cold finger which was in turn cooled by liquid nitrogen drawn from a cryostat as shown in Fig. 4. By controlling the supply of liquid nitrogen coolant and the size of the cold finger, sample cooling rates in the range 0.1 to 5°C/min could be obtained and the transition appeared as a sharp spike on the cooling curve. A copper/constantan thermocouple located in the toluene coolant indicated that the cooling was proceeding at the desired rate; it was switched off when the temperature approached the calibrated range of the thermistor. Heat losses from the outer calorimeter were kept constant by placing the calorimeter in an ice–water slurry.

The microcalorimeter was calibrated with 25 runs, the amount of water in it varying from 5–400 mg. A typical response curve is shown in Fig. 5(a). Some supercooling occurred and the

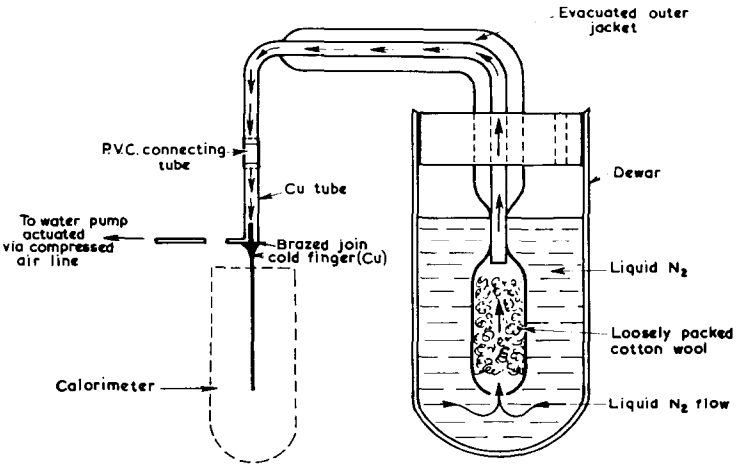

FIG. 4. Cryostat.

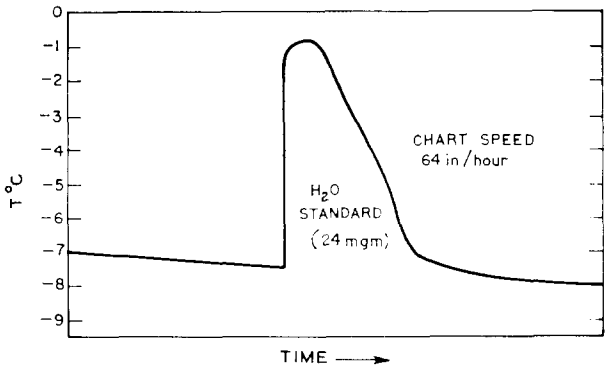

FIG. 5. (a) Response curve of microcalorimeter for water calibration.

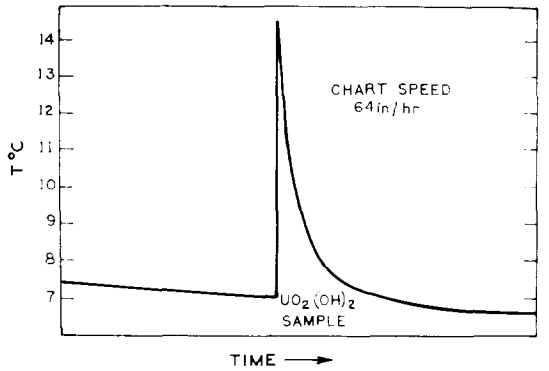

FIG. 5. (b) Response curve of microcalorimeter for β-$UO_2(OH)_2$ sample.

peaks became broader as the mass of water increased. The mean ice transformation temperature was −5°C, about 10° lower than the phase transition. A 7° rise in temperature at the transition was obtained with a 10 mg sample.

The heat of the ice–water transformation at 0°C is 79.8 cal/g. The heat of transformation at −5°C is, by the Kirchoff equation, $79.8 - 5(s_{water} - s_{ice})$ where s is the specific heat. Using $\Delta s = 0.518$ (*9*), the corrected heat of transformation is 77.2 cal/g. The heat evolved in the calorimeter was thus $77.2\, m_w$, where m_w is the mass of water. The area A under the response curve was assumed to be proportional to the temperature rise, with proportionality constant k. Therefore,

$$77.2\, m_w = kA(m_w s_I + W),$$

where W is the water equivalent of the calorimeter and s_I is the specific heat of ice (at about −5°C the water abruptly turns to ice). The curve of A vs. m_w is given in Fig. 6. An iterative procedure gave $\bar{k} = 100 \pm 14$ and $\bar{W} = 0.082 \pm 0.013$ cal/deg.

Calorimeter Results

The heat of transformation for the $\beta \rightarrow \alpha$ transition in $UO_2(OH)_2$ was measured by introducing about 0.2 g of the β phase and 0.06 g of toluene into the inner calorimeter. The heat output was similar to the output from 6 mg of water; this position is marked with an arrow in Fig. 6. A typical response curve for a β-$UO_2(OH)_2$ sample is shown in Fig. 5(b). Assuming that the calibration constants $\bar{k}$ and $\bar{W}$ are applicable at the transition point, the heat of transformation H is given by:

$$H = M\bar{k}A(\bar{W} + s_T m_T + s_{UO_2(OH_2)} m_{UO_2(OH)_2})/ 1000\, m_{UO_2(OH)_2}\, c \text{ kcal/mole}$$

where M is the molecular weight of $UO_2(OH)_2$, s_T is the specific heat of toluene, m_T is the mass of toluene, $s_{UO_2(OH)_2}$ is the specific heat of the final (α,β) mixture, and $m_{UO_2(OH)_2}$ is the initial mass of β-$UO_2(OH)_2$. s_T was taken as 0.39 cal/deg/g (*9*) and $s_{UO_2(OH)_2}$ was estimated from a plot of s vs. ρ for the uranium compounds listed by Rand and Kubaschewski (*10*). The value of $s_{UO_2(OH)_2}$ used was 0.073 ± 0.010 cal/deg/g. c is the conversion factor used.

The calorimeter results are given in Table IV. The conversion factors used in the calculations

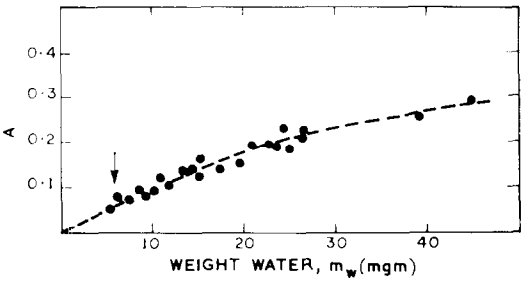

FIG. 6. Calibration curve for microcalorimeter.

TABLE IV

CALORIMETER RESULTS

Sample	C	C''	m_T (g)	$m_{UO_2(OH)_2}$ (g)	A	H (kcal/mole)
1	0.91	0.87	0.061	0.186	0.063	1.38
2	0.80	0.85	0.073	0.188	0.070	1.71
3	0.80	0.91	0.040	0.188	0.062	1.31
4	0.85	—	0.054	0.191	0.058	1.27
5	0.88	0.76	0.081	0.188	0.050	1.25
6	0.78	0.83	0.047	0.187	0.051	1.18
7	0.80[a]	—	0.045	0.185	0.054	1.24
8	0.80[a]	—	0.055	0.183	0.052	1.26
9	0.80[a]	—	0.072	0.183	0.064	1.64

[a] Not measured. Average value taken.

were the mean of direct weighing and X-ray determinations. The heat of transition found, $H = 1.36 \pm 0.18$ kcal/mole was large, indicating a large structural change (cf. latent heat of fusion of ice, 1.44 kcal/mole). Averaging all the transition temperatures in the dilatometric and calorimetric work gave a transition temperature of 5.1 ± 2.3°C. The percentage error in H as estimated from the probable errors in c (10%) and kW (16%), the main error producing terms, is 19%, giving a value of H of 1.36 ± 0.22 kcal/mole, and the latter error was adopted.

The large heat of transformation indicates that the transition is not a simple displacement one, as suggested by Harris and Taylor (*6*). For this type of transformation, e.g., the rhombic–monoclinic transition in sulphur (*11*), the enthalpy change is lower, about 0.1 kcal/mole.

Orientation Relationships

In the transformed samples a partly transformed crystal was occasionally observed. A photomicrograph (Fig. 7), taken with reflected polarized light, shows a β-$UO_2(OH)_2$ crystal on the left, three partly transformed crystals in the centre, and an α crystal on the right. The α and β forms are recognised by their different interedge angles. The line of demarcation of the α- and β-$UO_2(OH)_2$ phases in the partly-transformed crystals is sharp and lies in a diagonal plane since the edges of the two phases are of the type {111}. The morphological aspects of the bicrystal are shown in Fig. 8.

It was of great interest to note that the α product in the bicrystals showed complete extinction under crossed Nicols; thus the transformations, as far as they had gone, produced single crystals of the α phase. The α and β components had their pinacoidal faces roughly coplanar.

Type of Transformation

Polymorphism in inorganic and organic crystals usually involves slight displacements or molecular reorientations, magnetic ordering, Schottky effects, ferroelectric reversals, etc. The $\beta \rightarrow \alpha$ transformation in $UO_2(OH)_2$, however, is unusual in that it is analogous to the well known martensitic transformations of metals and alloys.

The main features of martensitic transformations are:

(i) They occur through the operation of a progressive shear through the crystal at near sonic speeds and are frequently accompanied by audible "clicks". A diffusion mechanism is not involved.
(ii) There is a temperature hysteresis.
(iii) Pressure as well as temperature is effective in actuating the transformation.
(iv) There is a specific orientation relation between parent and product lattices, and the shape change is the cause of the shear component.

All these are present in the $UO_2(OH)_2$ transformation:

(a) Audible "clicks" occur.
(b) The hysteresis is infinite as the α form cannot be reconverted into the β form by

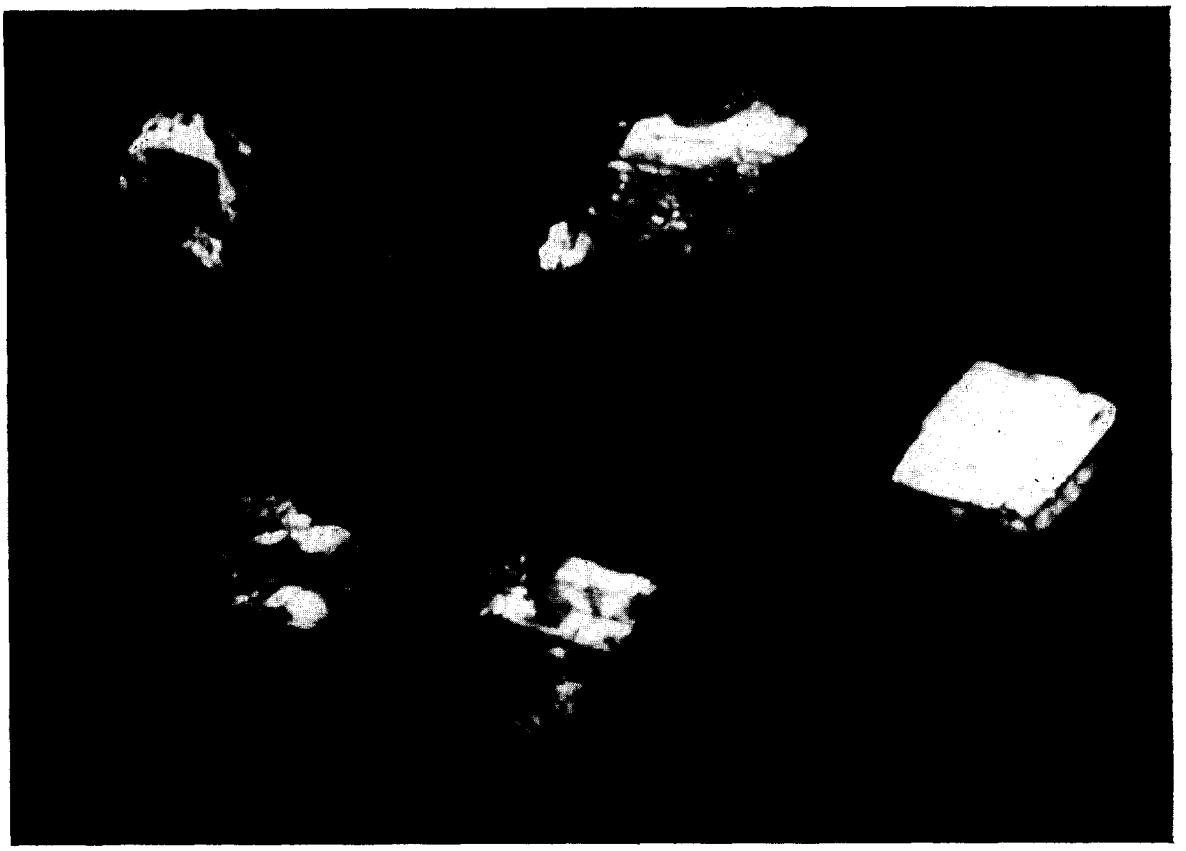

FIG. 7. Partly-transformed crystals.

heating. This may be due to the hydrogen bonds. In metals, the hysteresis is finite.

(c) Pressure as well as temperature is effective (*6*).

(d) A definite orientation relation occurs, which was discussed in the previous section.

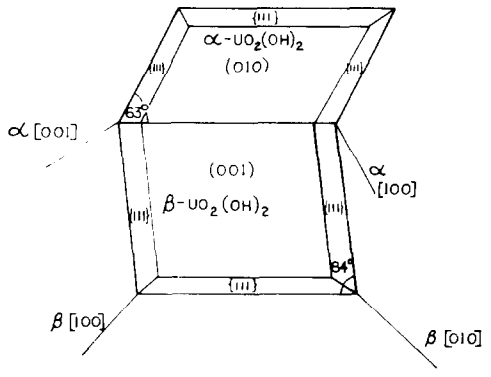

FIG. 8. Morphological aspects of partly-transformed crystal.

The present volume change of −14.7% is large compared with the changes of −1.12 and −0.70% for the $\beta \rightarrow \alpha$ and $\gamma \rightarrow \beta$ martensitic transformations in uranium (*12*). The present enthalpy change, 1.36 ± 0.22 kcal/mole is also large compared with the changes of 0.7 and 1.1 kcal/mole for the above uranium transitions. It is similar, however, to the enthalpy change of 1.42 kcal/mole for the high temperature monoclinic ↔ tetragonal transition in zirconia (*13*), which is also martensitic.

Proposed Mechanism for the $UO_2(OH)_2$ Transformation

With the aid of the structural data of Bannister and Taylor (*3*), a mechanism for the transformation in the region of nucleation is proposed.

The octahedra in the layer $Z = 0$ of β-$UO_2(OH)_2$ are shown in Fig. 9. The hydroxyl oxygens O(2), on the corners of the octahedra, are up or down from this plane by 1 Å, and the uranyl oxygens, O(1), at the apices by 1.5 Å.

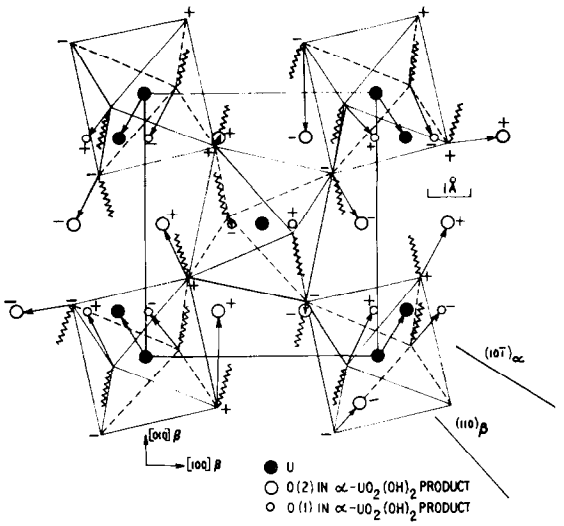

FIG. 9. The layer $Z = 0$ of the β-$UO_2(OH)_2$ structure. Arrows indicate shifts producing the layer $y = 0$ of the α-$UO_2(OH)_2$ phase, and springs denote the hydrogen bonds. + and − signs denote locations above and below the layer.

The + and − signs indicate that the atom concerned is up or down. Superimposed on this diagram are circles representing the atoms in a $y = 0$ layer of α-$UO_2(OH)_2$. The hydroxyl and uranyl oxygen atoms in α-$UO_2(OH)_2$ are practically the same distances above and below the plane as in β-$UO_2(OH)_2$. The α-phase orientation is such that the α- and β-phase diagonal planes are nearly coplanar, as suggested by the morphology in Fig. 8. The arrows indicate shifts to be applied to the β-phase atoms to produce the α phase. Important aspects of the shifts are:

(i) β-$UO_2(OH)_2$ atoms lying below the plane $Z = 0$ are still below it by the same amount after moving, and similarly for the β-$UO_2(OH)_2$ atoms above the plane.
(ii) The hydrogen bonds are marked as springs in Fig. 9. It is seen that the movements are generally in the direction of pull of the hydrogen bonds.
(iii) The atomic movements are a general collapse into the holes of the open β-$UO_2(OH)_2$ structure.

Thus it appears that as the β-$UO_2(OH)_2$ phase is cooled, the strength of the hydrogen bonds outweighs the effect of the thermal vibrations stabilising the β-$UO_2(OH)_2$ structure.

It was observed that the α-$UO_2(OH)_2$ components of the partly transformed crystals in Fig. 8 were single crystals. This suggested that in the overall transformation the hydrogen bonds were not broken, otherwise shattering should occur. In Fig. 10, the layer at $Z = \frac{1}{2}$ of β-$UO_2(OH)_2$ is shown. Atomic shifts which are symmetry related to those in Fig. 9 are shown producing the $y = \frac{1}{2}$ layer of the α-$UO_2(OH)_2$ product. In addition, the shifts of the oxygen atoms in adjoining layers (at $Z = 0$ or $Z = 1$), to which these atoms are hydrogen bonded, are shown.

In Fig. 10, the springs represent hydrogen bonds in projection; at the ends are O(1) and O(2) atoms. For any hydrogen bond, the ends of the arrows represent the new O(1) and O(2) positions, after the transformation. As the distances between the ends of the arrows are the same as the original length of the spring, the hydrogen bond distances are preserved. Since in both phases the O–H vectors are nearly perpendicular to the $UO_2(OH)_2$ layers, the hydrogens follow together with the O(2) atoms and remain associated with the same hydrogen bond. These considerations support our earlier conclusion that hydrogen bonds are not broken in the transformation. A slip of 1 Å between the α-$UO_2(OH)_2$ layers in Figs. 9 and 10 is needed

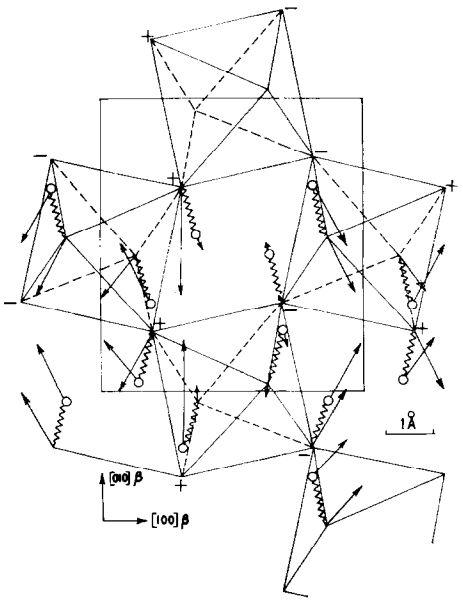

FIG. 10. The layer $Z = \frac{1}{2}$ of the β-$UO_2(OH)_2$ structure, with shifts symmetry related to Fig. 9, producing the layer $y = \frac{1}{2}$ of the α-$UO_2(OH)_2$ phase. o—Hydrogen-bonded oxygen in adjacent layer.

to produce the orthogonality of the α-$UO_2(OH)_2$ lattice.

It is suggested that the transformation starts at a nucleation centre where the hydrogen bond strength is sufficient to overcome the thermal vibrations and collapse atoms into the holes in the β-$UO_2(OH)_2$ lattice, in the manner shown in Figs. 9 and 10. The transformation is propagated through the crystal by a shear or buckling process which enables the β phase to assume the correct orientation relative to the produce phase.

Acknowledgments

We would like to thank Dr. C. J. Hardy and Dr. M. J. Bannister for helpful comments, and Mr. E. Meller for producing Fig. 7.

References

1. J. K. Dawson, E. Wait, K. Alcock, and D. R. Chilton, *J. Chem. Soc.* 3531 (1956).
2. R. B. Roof, Jr., D. T. Cromer, and A. C. Larson, *Acta Crystallogr.* **17**, 701 (1964).
3. M. J. Bannister and J. C. Taylor, *Acta Crystallogr.* **B26**, 1775 (1970).
4. J. C. Taylor, *Acta Crystallogr.* **B27**, 1088 (1971).
5. J. C. Taylor and H. J. Hurst, *Acta Crystallogr.*, **B27**, 2018 (1971).
6. L. A. Harris and A. J. Taylor, *J. Amer. Ceram. Soc.* **45**, 25 (1962).
7. G. W. Brindley, *Phil. Mag.* **36**, 347 (1945).
8. "International Tables for X-Ray Crystallography," Vol. III, p. 195, Kynoch Press, Birmingham (1962).
9. "Handbook of Chemistry and Physics 51st Ed.," Chemical Rubber Co., Cleveland, Ohio (1970).
10. M. H. Rand and O. Kubaschewski, "The Thermo-Chemical Properties of Uranium Compounds," Interscience, New York (1963).
11. E. D. West, *J. Amer. Chem. Soc.* **81**, 29 (1959).
12. P. Chiotti, H. H. Klepfer, and R. W. White, *Trans. Amer. Soc. Met.* **51**, 772 (1959).
13. G. M. Wolten, *J. Amer. Ceram. Soc.* **46**, 418 (1963).